Electronic Supplementary Material (ESI) for Nanoscale.

Supporting Information

Electronic Properties of Polymorphic Two-Dimensional Layered Chromium Disulphide

Mohammad Rezwan Habib,[a #] Shengping Wang,[b #] Weijia Wang,[a] Han Xiao,[a] Sk Md Obaidulla,[a] Anabil Gayen,[a] Yahya Khan,[a] Hongzheng Chen,[b] and Mingsheng Xu[a*]

[a] State Key Laboratory of Silicon Materials, College of Information Science & Electronic Engineering, Zhejiang University, Hangzhou 310027, P. R. China.

[b] Department of Polymer Science and Engineering, Zhejiang University, Hangzhou 310027, P. R. China.

* Corresponding author: msxu@zju.edu.cn

[#] These authors contributed equally to this work

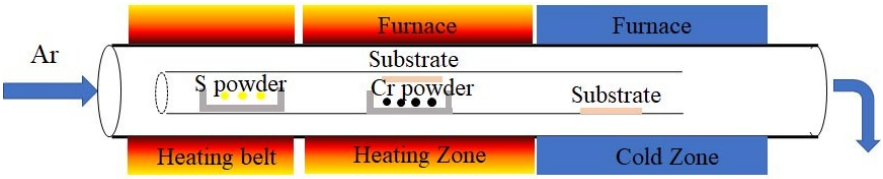

Fig. S1 (a) Schematic illustration of CVD system for 2D layered CrS_2 synthesis.

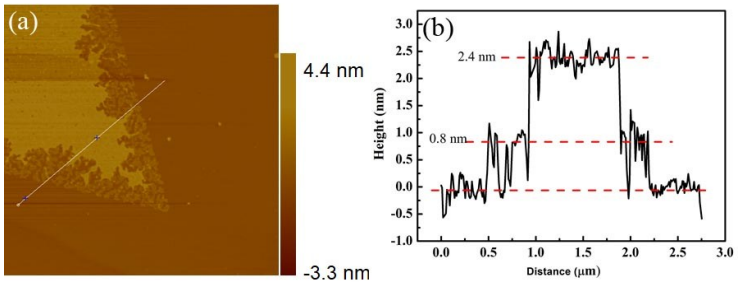

Fig. S2 (a) AFM topological image of CrS_2 flake. (b) The height profile taken across the line in (a). The results show a layered structure of our 2D CrS_2 flake.

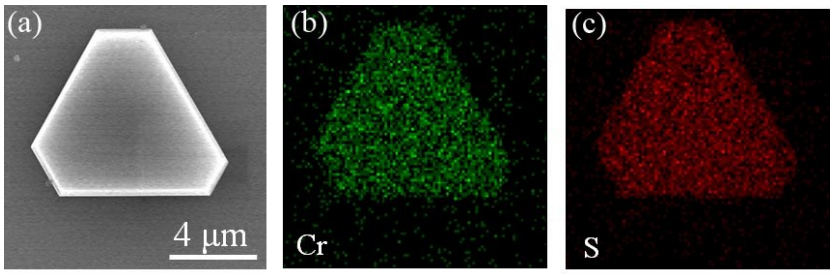

Fig. S3 (a) SEM image of a CrS_2 flake. Corresponding EDX mapping of (b) Cr and (c) S, suggesting quite uniform distribution of the Cr and S elements in the flake.

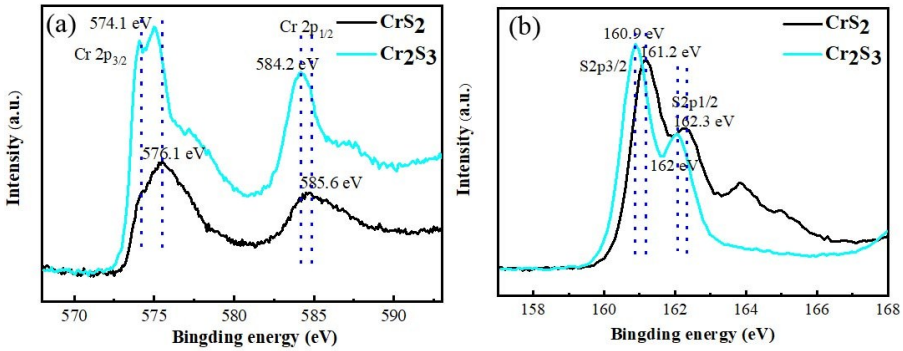

Fig. S4 Comparison of XPS patterns of Cr 2p and S 2p for the Cr_2S_3 powder and our CrS_2 sample. (a) Cr 2p patterns. (b) S 2p patterns. The energies were calibrated as C 1s peak as 284.5 eV.

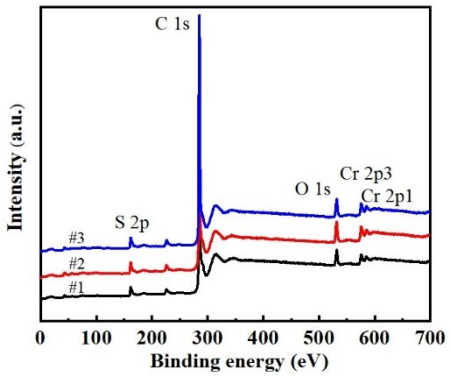

Fig. S5 XPS patterns of CrS_2 collected at different measurement positions.

Table S1. Atomic percentage (atomic %) of the sample based on the measurements in Fig. S5.

Measurement	C 1s	O 1s	S 2p	Cr 2p	Cr 2p/S 2p
#1	93.2%	3.7%	2.1%	1.0%	1.0 : 2.1
#2	91.7%	4.5%	2.5%	1.3%	1.0 : 1.92
#3	92.6%	4.0%	2.3%	1.1%	1.0 : 2.09

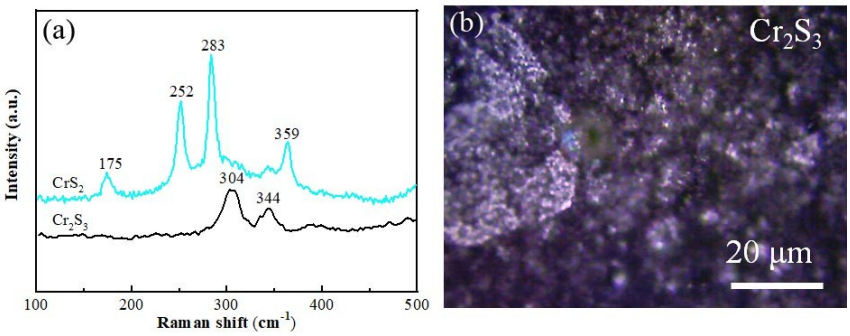

Fig. S6 (a) Comparison of Raman scatterings of our CrS_2 and Cr_2S_3 powder. (b) Optical image shows where the Raman spectrum of Cr_2S_3 was obtained.

A. Comparison of Raman characteristics of our 2D layered CrS_2 to non-layered Cr_2S_3

Very recently, Zhou et al.[1] reported synthesis of 2D non-layered Cr_2S_3 and characterized it by Raman technique in details. They found that the Cr_2S_3 ultrathin flakes have six Raman modes labeled as P1 (~175.7 cm^{-1}), P2 (~247.4 cm^{-1}), P3 (~281 cm^{-1}), P4 (~304.6 cm^{-1}), P5 (~337.9 cm^{-1}), and P6 (~355.5 cm^{-1}), respectively. Among these six Raman modes, P1, P2, P3, P6 have relatively distinguishable intensity. They also found that for the non-layered rhombohedral Cr_2S_3, the abnormal red-shift of the P2, P3, P6 modes (no change of P1) with increase in the thickness is mainly attributed to the change of covalent bond strength between Cr and S atoms coming from the stacking effect.

Besides the Raman spectrum presented in main text, we here show the Raman spectrum of another CrS_2 flake (few layer) with a different thickness from that (about 6.4 nm) in

the main text. The peaks of Raman modes of our sample are at about 175 cm^{-1}, 252 cm^{-1}, 283 cm^{-1} and 359 cm^{-1} (Fig. S7). And the Raman modes of our Cr_2S_3 powder are at about 304 cm^{-1} and 344 cm^{-1}. These compounds containing Cr and S have some similar Raman features, but they show distinguishing characteristics from each other. As mentioned above, the different covalent bond strength between Cr and S atoms influences the Raman shift. Thus, the different positions of Raman peaks of our CrS_2 sample from the Cr_2S_3 ultrathin film is reasonable. In addition, the discussion of the layer-dependent Raman features and the assignment/identification of the modes of our 2D CrS_2 are beyond the scope of the present work.

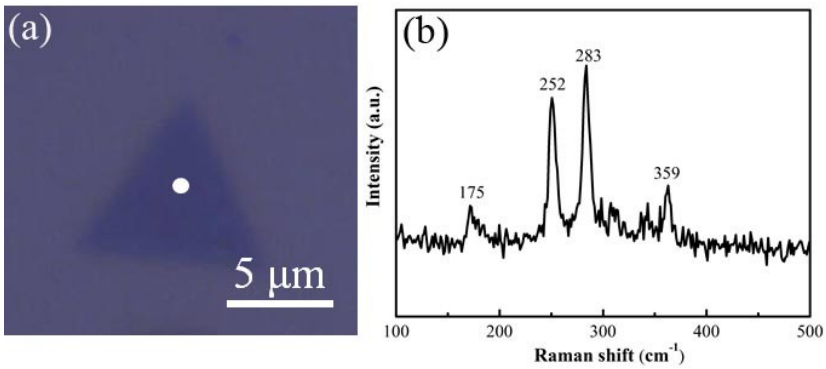

Fig. S7 (a) Optical image of a CrS_2 flake. (b) Raman spectrum collected at the white dot position in (a).

Table S2. Summary of Raman peak positions of different samples.

Sample\Raman mode (cm^{-1})	**P1**	**P2**	**P3**	**P4**	**P5**	**P6**
Non-layered Cr_2S_3 (Adv. Funct. Mater. **2019**, *29,* 1805880.) (laser λ = 633 nm)	175.7	247.4	281	304.6	337.9	355.5
Our CrS_2 (laser λ = 532 nm)	175.0	252.0	283.0			359.0
$\Delta = R_{CrS2} - R_{Cr2S3}$	**-0.7**	**4.6**	**2.0**			**3.5**
Our Cr_2S_3 powder (laser λ = 532 nm)				304.0	344	
arXiv:1805.08002 (laser λ = 455 nm)		254	286			

Note: The $\Delta = R_{CrS2} - R_{Cr2S3}$ is the difference of the Raman shift at specific peaks between our CrS_2 and Cr_2S_3. We find that there is no an identical change trend among the peaks.

B. Effect of Raman excitation wavelength on Raman scattering

The Raman spectrum study for TMDs such as MoS_2 has been normally done with the standard green excitation (514 - 532 nm) or in resonant conditions (633 nm). And the existence of a resonant excitation of several peaks when using 633 nm, 785 nm and 325 nm excitation wavelengths is related to electron-phonon coupling with different transitions in the MoS_2 energy band structure. Despite this, the peak positions of the two very intense peaks at 382.9 and 408.1 cm^{-1} of bulk MoS_2, attributed to E_2g^1 and A_1g vibration mode, respectively, showed negligible shift with different excitation wavelengths.[2] However, if the sample is very thin such as monolayer WS_2, the frequencies of the Raman modes would change slightly (within 2 cm^{-1}) with a change in laser wavelength.[3] The reasons for this may be due to the increase in lattice temperature by strong optical absorption and the modification of force constants of the

vibration by photo-excited carriers.[4]

The comparison confirms that our samples show some characteristics of the compounds comprising of Cr and S, but our 2D layered CrS_2 has its own Raman features due to its structure.

C. Raman spectra from DFPT calculation and comparison with Raman spectra of CVD grown CrS_2

The Raman spectra for the polymorphs of CrS_2 are executed from density functional perturbation theory (DFPT) as implemented in the CASTEP package.[5] For the CASTEP computation we have used the VASP optimized structures with a similar k-point mesh as input with Norm-conserving pseudopotentials (energy cut-off 700 eV) and PBE version of GGA exchange correlation functional. Before DFPT calculation, full geometry optimization was performed and both code gave almost same lattice parameter and atomic positions.

The Raman spectra of three phases of CrS_2 are shown in Fig. S8. The calculated Raman modes of each phase of CrS_2 are mentioned inside the Fig. S8**.** The calculated Raman modes for 1T and 1T' phases are matched with the experimental Raman mode. In general, the calculated Raman shift underestimate the experimental Raman shift.[6] The calculated Raman modes of 2H phase are at 391.4 cm^{-1} and 405.6 cm^{-1} and those peaks are very low in intensity as observed in experimental Raman spectra. From this comparison (Table S3), we can conclude that the three phases coexist in our CVD grown CrS_2. Moreover, such low intensity of the characteristics peaks of semiconducting 2H phase indicates the presence of small percentage in the CVD grown CrS_2.

Table S3: Comparison of theoretical and experimental Raman peaks of CrS_2

Theoretical (Cm^{-1})			Experimental (Cm^{-1})
2H-CrS_2	**1T-CrS_2**	**1T'-CrS_2**	**As prepared CrS_2 sample**
		187.6	175
	244.7	243.0	252
		285.9	283
		353.8	346.5
	361		359
391.4			385
405.6		405.6	403
		453.9	

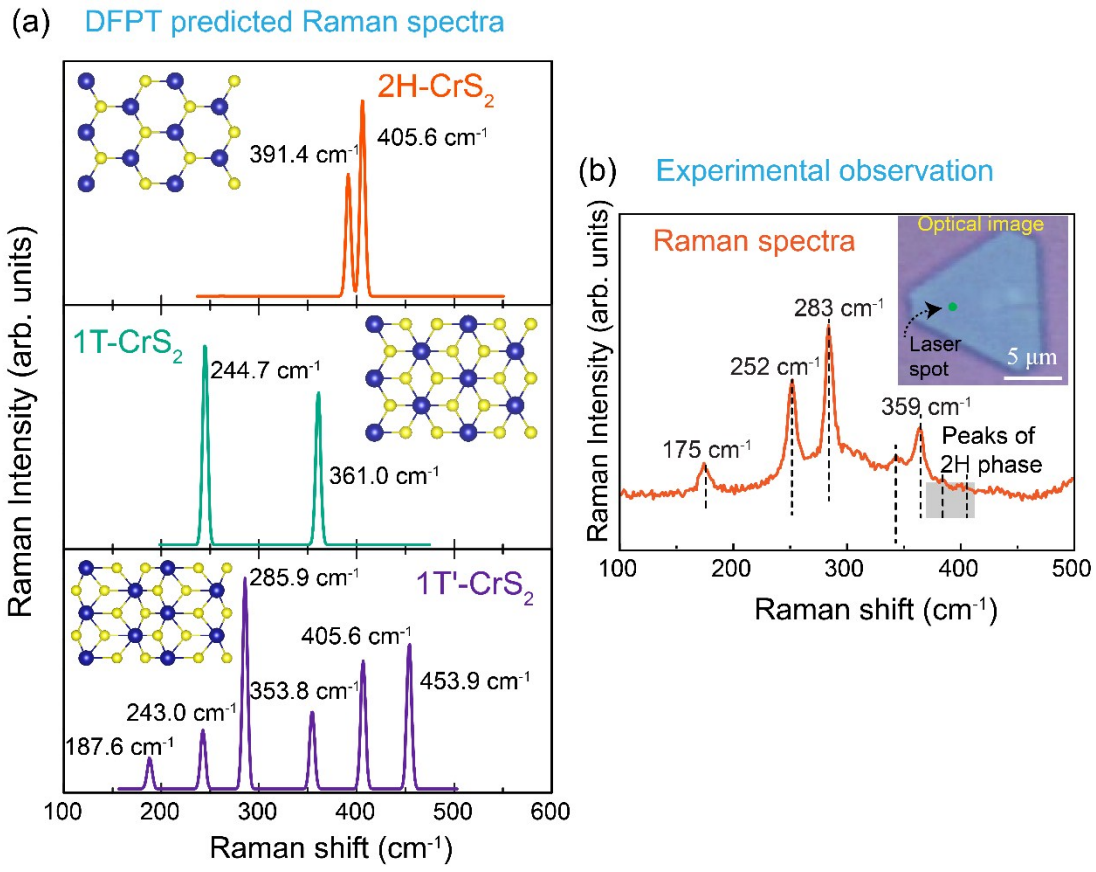

Fig. S8 (a) Raman spectra of three different phases of CrS_2 predicted from DFPT calculation. (b) Raman spectra of CVD grown CrS_2 film (as depicted inset).

D. The analysis of crystallographic structure of 2D layer CrS_2 by comparing to the known compounds containing Cr and S

Our samples both on Si with diffraction peak at about 33° and on Al_2O_3 with diffraction peak at 37° substrates have an identical diffraction peak at 2θ of about 15°. We find that for other 2D layered TMDs such as MoS_2 and WS_2, they also show a diffraction peak at about 14° - 15°, belonging to the (002).[7, 8] The interplanar spacings from the SAED are about 0.2941 nm (d_1) and 0.1723 nm (d_2) (Fig. S9), which are not matched with those in PDF (Powder Diffraction File) of the compounds containing Cr and S (Fig. S10-S15)

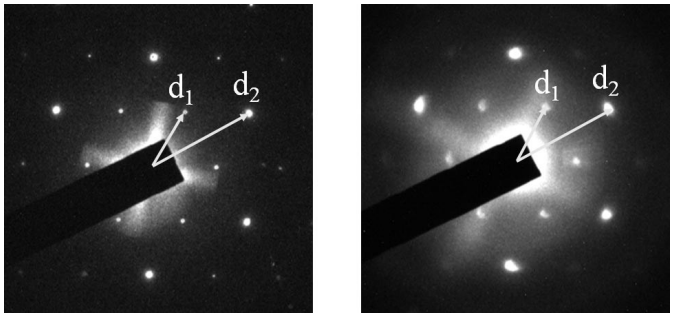

Fig. S9 SAED patterns for different CrS_2 flakes.

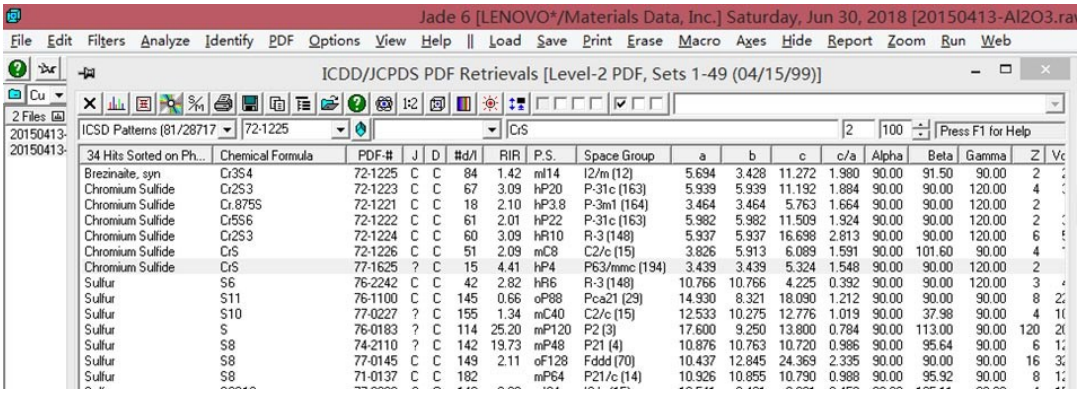

Fig. S10 The PDF information about the known compounds comprising Cr and S.

The PDF information of the compounds containing Cr and S for Cr_3S_4 (PDF # 72-1225) (Fig. S10), Cr_2S_3 (PDF # 72-1223, and PDF # 72-1224) (Fig. S11), $Cr_{.875}S$ (PDF # 72-1221) (Fig. S12), Cr_5S_6 (PDF # 72-1222) (Fig. S13) and CrS (PDF # 72-1225, PDF #

72-12262) (Fig. S14) are below for reference.

Reference | Lines(97) | PDF2

#	2-Theta	d(?)	I(f)	(h k l)	Theta	1/(2d)	2pi/d	n
1	15.716	5.6341	71.1	(0 0 2)	7.858	0.0887	1.1152	
2	17.254	5.1350	25.3	(-1 0 1)	8.627	0.0974	1.2236	
3	17.625	5.0279	54.8	(1 0 1)	8.812	0.0994	1.2497	
4	27.168	3.2796	19.4	(0 1 1)	13.584	0.1525	1.9158	
5	28.095	3.1734	11.8	(-1 0 3)	14.048	0.1576	1.9799	
6	28.794	3.0979	17.7	(1 0 3)	14.397	0.1614	2.0282	
7	30.414	2.9366	45.9	(1 1 0)	15.207	0.1703	2.1396	
8	31.406	2.8460	25.7	(2 0 0)	15.703	0.1757	2.2077	
9	31.738	2.8170	2.0	(0 0 4)	15.869	0.1775	2.2304	
10	34.214	2.6186	100.0	(-1 1 2)	17.107	0.1909	2.3994	
11	34.607	2.5898	18.6	(1 1 2)	17.303	0.1931	2.4261	
12	34.917	2.5675	10.3	(-2 0 2)	17.458	0.1947	2.4472	
13	35.422	2.5320	29.4	(0 1 3)	17.711	0.1975	2.4815	
14	35.685	2.5140	49.8	(2 0 2)	17.842	0.1989	2.4993	
15	42.164	2.1414	5.8	(2 1 1)	21.082	0.2335	2.9341	
16	42.729	2.1144	0.1	(-1 0 5)	21.365	0.2365	2.9716	
17	43.541	2.0768	1.1	(1 0 5)	21.770	0.2407	3.0253	
18	44.215	2.0468	89.2	(-1 1 4)	22.107	0.2443	3.0698	
19	44.626	2.0288	31.7	(-2 0 4)	22.313	0.2464	3.0969	
20	44.848	2.0193	72.2	(1 1 4)	22.424	0.2476	3.1116	
21	45.876	1.9764	39.5	(2 0 4)	22.938	0.2530	3.1791	
22	47.607	1.9085	15.9	(-2 1 3)	23.803	0.2620	3.2922	
23	48.503	1.8753	7.9	(2 1 3)	24.251	0.2666	3.3504	
24	48.844	1.8630	1.3	(3 0 1)	24.422	0.2684	3.3725	
25	53.411	1.7140	35.6	(0 2 0)	26.706	0.2917	3.6658	
26	54.723	1.6760	0.8	(3 0 3)	27.361	0.2983	3.7490	
27	55.293	1.6600	55.6	(3 1 0)	27.646	0.3012	3.7850	
28	56.035	1.6398	2.7	(0 2 2)	28.017	0.3049	3.8317	
29	56.560	1.6258	1.3	(-1 2 1)	28.280	0.3075	3.8646	
30	56.692	1.6223	3.0	(1 2 1)	28.346	0.3082	3.8729	
31	57.465	1.6023	2.5	(-3 1 2)	28.733	0.3120	3.9213	
32	57.876	1.5919	2.2	(-1 1 6)	28.938	0.3141	3.9469	

Fig. S11 PDF # 72-1225 of Cr_3S_4.

Reference | Lines(68) | PDF2

#	2-Theta	d(?)	I(f)	(h k l)	Theta	1/(2d)	2pi/d	n^
1	15.824	5.5960	41.8	(0 0 2)	7.912	0.0893	1.1228	
2	17.226	5.1433	6.3	(1 0 0)	8.613	0.0972	1.2216	
3	18.974	4.6734	29.0	(1 0 1)	9.487	0.1070	1.3444	
4	23.473	3.7868	5.3	(1 0 2)	11.736	0.1320	1.6592	
5	29.555	3.0199	8.1	(1 0 3)	14.778	0.1656	2.0806	
6	30.069	2.9695	22.2	(1 1 0)	15.034	0.1684	2.1159	
7	31.959	2.7980	0.2	(0 0 4)	15.980	0.1787	2.2456	
8	34.154	2.6231	100.0	(-1-1 2)	17.077	0.1906	2.3954	
9	34.858	2.5717	1.2	(2 0 0)	17.429	0.1944	2.4432	
10	35.797	2.5064	4.4	(2 0 1)	17.898	0.1995	2.5069	
11	36.528	2.4578	1.4	(1 0 4)	18.264	0.2034	2.5564	
12	38.494	2.3367	1.1	(2 0 2)	19.247	0.2140	2.6889	
13	42.667	2.1174	2.4	(2 0 3)	21.333	0.2361	2.9675	
14	44.085	2.0524	3.2	(1 0 5)	22.043	0.2436	3.0613	
15	44.451	2.0364	94.0	(-1-1 4)	22.225	0.2455	3.0854	
16	46.686	1.9440	0.6	(2 1 0)	23.343	0.2572	3.2321	
17	47.428	1.9153	3.3	(-2-1 1)	23.714	0.2611	3.2805	
18	48.011	1.8934	0.5	(2 0 4)	24.005	0.2641	3.3184	
19	48.780	1.8653	1.3	(0 0 6)	24.390	0.2680	3.3684	
20	49.602	1.8363	0.9	(-2-1 2)	24.801	0.2723	3.4216	
21	52.114	1.7536	0.4	(1 0 6)	26.057	0.2851	3.5831	
22	53.078	1.7240	2.7	(-2-1 3)	26.539	0.2900	3.6446	
23	53.396	1.7144	40.6	(3 0 0)	26.698	0.2916	3.6649	
24	54.287	1.6884	1.1	(2 0 5)	27.143	0.2961	3.7214	
25	56.056	1.6392	4.5	(3 0 2)	28.028	0.3050	3.8330	
26	57.695	1.5965	0.6	(-2-1 4)	28.848	0.3132	3.9356	
27	58.374	1.5796	13.8	(-1-1 6)	29.187	0.3165	3.9778	
28	60.598	1.5268	0.6	(1 0 7)	30.299	0.3275	4.1153	
29	61.346	1.5100	0.2	(2 0 6)	30.673	0.3311	4.1612	
30	62.503	1.4848	1.6	(2 2 0)	31.251	0.3368	4.2318	
31	63.310	1.4677	1.0	(-2-1 5)	31.655	0.3407	4.2809	
32	63.596	1.4618	0.2	(3 0 4)	31.798	0.3420	4.2981	
33	64.924	1.4351	9.1	(-2-2 2)	32.462	0.3484	4.3782	

Reference | Lines(60) | PDF2

#	2-Theta	d(?)	I(f)	(h k l)	Theta	1/(2d)	2pi/d	n^2
1	15.909	5.5660	41.1	(0 0 3)	7.955	0.0898	1.1289	
2	18.037	4.9139	22.1	(1 0 1)	9.019	0.1018	1.2787	
3	20.267	4.3780	16.1	(0 1 2)	10.134	0.1142	1.4352	
4	27.499	3.2408	6.7	(1 0 4)	13.750	0.1543	1.9388	
5	30.079	2.9685	22.1	(1 1 0)	15.039	0.1684	2.1166	
6	31.928	2.8007	4.2	(0 1 5)	15.964	0.1785	2.2435	
7	34.205	2.6193	100.0	(1 1-3)	17.102	0.1909	2.3988	
8	35.295	2.5409	3.2	(0 2 1)	17.647	0.1968	2.4729	
9	36.542	2.4570	2.7	(2 0 2)	18.271	0.2035	2.5573	
10	41.206	2.1890	1.8	(0 2 4)	20.603	0.2284	2.8703	
11	41.706	2.1639	1.7	(1 0 7)	20.853	0.2311	2.9037	
12	44.592	2.0303	93.0	(1 1-6)	22.296	0.2463	3.0947	
13	46.943	1.9340	1.4	(0 1 8)	23.471	0.2585	3.2489	
14	47.037	1.9303	2.7	(2 1 1)	23.518	0.2590	3.2550	
15	48.029	1.8927	2.1	(2 1-2)	24.014	0.2642	3.3196	
16	49.060	1.8553	1.3	(0 0 9)	24.530	0.2695	3.3866	
17	51.853	1.7618	1.6	(1 2-4)	25.926	0.2838	3.5664	
18	52.273	1.7486	0.8	(0 2 7)	26.136	0.2859	3.5932	
19	53.416	1.7139	40.5	(3 0 0)	26.708	0.2917	3.6661	
20	54.593	1.6797	1.3	(2 1-5)	27.296	0.2977	3.7407	
21	56.103	1.6380	4.4	(3 0 3)	28.051	0.3053	3.8360	
22	56.766	1.6204	0.6	(2 0 8)	28.383	0.3086	3.8775	
23	58.027	1.5882	0.6	(1 0 10)	29.014	0.3148	3.9563	
24	58.628	1.5733	13.7	(1 1-9)	29.314	0.3178	3.9936	
25	61.495	1.5066	0.8	(1 2-7)	30.747	0.3319	4.1703	
26	62.526	1.4842	1.6	(2 2 0)	31.263	0.3369	4.2332	
27	63.718	1.4593	0.2	(0 3 6)	31.859	0.3426	4.3055	
28	63.887	1.4559	0.4	(0 1 11)	31.944	0.3434	4.3158	
29	64.973	1.4341	9.1	(2 2-3)	32.487	0.3486	4.3812	
30	65.581	1.4223	0.8	(2 1-8)	32.791	0.3515	4.4176	
31	65.657	1.4209	0.8	(3 1-1)	32.828	0.3519	4.4221	

Fig. S12 PDF # 72-1223 and PDF # 72-1224 of Cr_2S_3.

Reference | Lines(18) | PDF2

#	2-Theta	d(?)	I(f)	(h k l)	Theta	1/(2d)	2pi/d	n^2
1	15.362	5.7630	0.1	(0 0 1)	7.681	0.0868	1.0903	
2	29.757	2.9999	39.2	(1 0 0)	14.878	0.1667	2.0945	
3	31.010	2.8815	2.2	(0 0 2)	15.505	0.1735	2.1805	
4	33.653	2.6610	51.4	(1 0 1)	16.826	0.1879	2.3612	
5	43.513	2.0781	100.0	(0 1 2)	21.756	0.2406	3.0235	
6	47.279	1.9210	0.1	(0 0 3)	23.639	0.2603	3.2708	
7	52.813	1.7320	38.1	(1 1 0)	26.406	0.2887	3.6277	
8	56.868	1.6177	7.5	(1 0 3)	28.434	0.3091	3.8839	
9	61.799	1.5000	2.9	(2 0 0)	30.899	0.3333	4.1889	
10	62.516	1.4845	1.1	(1 1 2)	31.258	0.3368	4.2326	
11	64.098	1.4516	4.8	(0 2 1)	32.049	0.3444	4.3285	
12	64.639	1.4408	5.8	(0 0 4)	32.319	0.3470	4.3611	
13	70.753	1.3305	14.6	(2 0 2)	35.376	0.3758	4.7225	
14	72.754	1.2987	2.8	(1 0 4)	36.377	0.3850	4.8379	
15	81.315	1.1823	2.0	(0 2 3)	40.658	0.4229	5.3146	
16	85.585	1.1339	1.4	(2 1 0)	42.792	0.4410	5.5414	
17	87.636	1.1125	3.3	(2 1 1)	43.818	0.4494	5.6477	
18	88.123	1.1076	10.6	(1 1 4)	44.062	0.4514	5.6726	

Fig. S13 PDF # 72-1221 of $Cr_{.875}S$.

Reference | Lines(15) | PDF2

#	2-Theta	d(?)	I(f)	(h k l)	Theta	1/(2d)	2pi/d	n^2
1	29.978	2.9783	56.3	(1 0 0)	14.989	0.1679	2.1097	
2	33.639	2.6620	4.0	(0 0 2)	16.820	0.1878	2.3603	
3	34.477	2.5992	46.8	(1 0 1)	17.239	0.1924	2.4173	
4	45.673	1.9848	100.0	(1 0 2)	22.836	0.2519	3.1657	
5	53.227	1.7195	42.8	(1 1 0)	26.613	0.2908	3.6541	
6	60.697	1.5245	5.7	(1 0 3)	30.348	0.3280	4.1214	
7	62.298	1.4891	4.1	(2 0 0)	31.149	0.3358	4.2194	
8	64.457	1.4444	2.1	(1 1 2)	32.228	0.3462	4.3501	
9	64.976	1.4341	4.4	(2 0 1)	32.488	0.3487	4.3813	
10	70.722	1.3310	4.5	(0 0 4)	35.361	0.3757	4.7207	
11	72.698	1.2996	15.8	(2 0 2)	36.349	0.3847	4.8347	
12	78.675	1.2152	2.9	(1 0 4)	39.337	0.4115	5.1706	
13	84.946	1.1407	1.7	(2 0 3)	42.473	0.4383	5.5080	
14	86.358	1.1257	4.0	(2 1 0)	43.179	0.4442	5.5817	
15	88.759	1.1013	3.0	(2 1 1)	44.380	0.4540	5.7051	

Fig. S14 PDF # 72-1222 of Cr_5S_6.

Reference | Lines(53) | PDF2

#	2-Theta	d(?)	I(f)	(h k l)	Theta	1/(2d)	2pi/d	n^2
1	28.167	3.1655	83.9	(1 1 0)	14.083	0.1580	1.9849	
2	29.591	3.0163	46.2	(-1 1 1)	14.796	0.1658	2.0831	
3	29.936	2.9823	9.9	(0 0 2)	14.968	0.1677	2.1068	
4	30.204	2.9565	22.9	(0 2 0)	15.102	0.1691	2.1252	
5	33.810	2.6489	21.6	(0 2 1)	16.905	0.1888	2.3720	
6	34.221	2.6181	28.5	(1 1 1)	17.110	0.1910	2.3999	
7	37.735	2.3820	100.0	(-1 1 2)	18.867	0.2099	2.6378	
8	43.045	2.0996	76.7	(0 2 2)	21.522	0.2381	2.9925	
9	45.133	2.0072	52.6	(1 1 2)	22.567	0.2491	3.1303	
10	48.542	1.8739	32.9	(2 0 0)	24.271	0.2668	3.3529	
11	49.802	1.8294	7.2	(-1 1 3)	24.901	0.2733	3.4345	
12	52.117	1.7535	2.3	(-2 0 2)	26.059	0.2852	3.5833	
13	52.406	1.7445	48.1	(1 3 0)	26.203	0.2866	3.6018	
14	53.269	1.7182	0.6	(-1 3 1)	26.635	0.2910	3.6568	
15	55.664	1.6499	3.4	(0 2 3)	27.832	0.3031	3.8083	
16	56.265	1.6336	0.4	(1 3 1)	28.132	0.3061	3.8461	
17	57.612	1.5986	3.0	(-2 2 1)	28.806	0.3128	3.9304	
18	58.243	1.5828	4.5	(2 2 0)	29.122	0.3159	3.9697	
19	58.712	1.5712	2.3	(-1 3 2)	29.356	0.3182	3.9989	
20	58.846	1.5680	4.7	(1 1 3)	29.423	0.3189	4.0072	
21	61.426	1.5082	19.4	(-2 2 2)	30.713	0.3315	4.1661	
22	62.204	1.4912	12.5	(0 0 4)	31.102	0.3353	4.2136	
23	62.809	1.4783	3.6	(0 4 0)	31.404	0.3382	4.2504	
24	63.239	1.4692	2.2	(2 2 1)	31.620	0.3403	4.2765	
25	63.688	1.4599	0.7	(2 0 2)	31.844	0.3425	4.3037	
26	64.323	1.4470	5.1	(1 3 2)	32.162	0.3455	4.3421	
27	64.323	1.4470	5.1	(-1 1 4)	32.162	0.3455	4.3421	
28	64.938	1.4348	3.1	(0 4 1)	32.469	0.3485	4.3790	
29	68.043	1.3767	0.2	(-1 3 3)	34.021	0.3632	4.5639	
30	69.255	1.3556	1.5	(-2 2 3)	34.628	0.3689	4.6352	
31	70.697	1.3314	2.0	(0 2 4)	35.349	0.3755	4.7192	

Reference | Lines(15) | PDF2

#	2-Theta	d(?)	I(f)	(h k l)	Theta	1/(2d)	2pi/d	n^2
1	29.978	2.9783	56.3	(1 0 0)	14.989	0.1679	2.1097	
2	33.639	2.6620	4.0	(0 0 2)	16.820	0.1878	2.3603	
3	34.477	2.5992	46.8	(1 0 1)	17.239	0.1924	2.4173	
4	45.673	1.9848	100.0	(1 0 2)	22.836	0.2519	3.1657	
5	53.227	1.7195	42.8	(1 1 0)	26.613	0.2908	3.6541	
6	60.697	1.5245	5.7	(1 0 3)	30.348	0.3280	4.1214	
7	62.298	1.4891	4.1	(2 0 0)	31.149	0.3358	4.2194	
8	64.457	1.4444	2.1	(1 1 2)	32.228	0.3462	4.3501	
9	64.976	1.4341	4.4	(2 0 1)	32.488	0.3487	4.3813	
10	70.722	1.3310	4.5	(0 0 4)	35.361	0.3757	4.7207	
11	72.698	1.2996	15.8	(2 0 2)	36.349	0.3847	4.8347	
12	78.675	1.2152	2.9	(1 0 4)	39.337	0.4115	5.1706	
13	84.946	1.1407	1.7	(2 0 3)	42.473	0.4383	5.5080	
14	86.358	1.1257	4.0	(2 1 0)	43.179	0.4442	5.5817	
15	88.759	1.1013	3.0	(2 1 1)	44.380	0.4540	5.7051	

Fig. S15 PDF # 72-1225 and PDF # 72-12262 of CrS.

E. Band structure using HSE06 functional

The computational expensive hybrid functional is mostly used to study the exact band position of 2D material. Here we also predicated the band structure of polymorphic CrS_2 using HSE06 functional. The 2H CrS_2 exhibit semiconducting behavior of direct band gap. The predicted band gap is ~1.47 eV which is ~0.5 eV larger than GGA+PBE predicted bandgap. The trigonal and distorted trigonal phase of CrS2 show metallic behavior (as shown in Fig. S16)

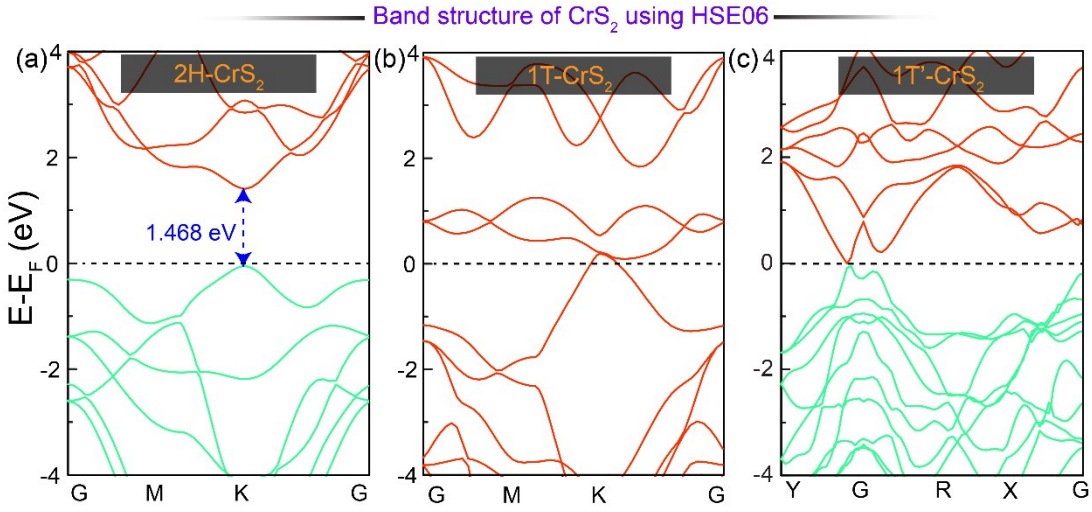

Fig. S16 Band structure of (a) 2H-CrS_2, (b) 1T-CrS_2, and (c) 1T'-CrS_2 using HSE06 functional. Black dotted line represent the Fermi level and set at 0 eV.

F. Spin polarized calculation and magnetic properties of polymorphic CrS_2

The spin polarized calculation has also been carried out to examine the magnetic behavior of polymorphic CrS_2. Table S4 shows the relative total energy with respect to the most stable phase with the same functional. For both spin polarized and non-spin polarized calculation within GGA functional the 2H phase is energetically stable. Moreover, the nonmagnetic 2H CrS_2 is energetically favorable and which is consistent with previous studies.[9, 10] After considering the onsite Coulomb U correction within GGA functional, the 1T'-CrS2 exhibit more stability than other two phases. The value of onsite Coulomb correction for Cr (U_{eff} =2.8) has been taken from previous literature.[9] Furthermore, we calculated the spin polarized DOS using GGA and GGA+U functional. The left panel of Fig. S17 depicts the spin polarized density of states of three phases without U correction and it shows that for three phases the DOS for spin up and spin down are equivalent and identical. From GGA predicted DOS, the polymorphic CrS_2 show nonmagnetic characteristics. But after considering the Hubbard correction (U), the spin polarized density of states for 1T and 1T' phase of CrS2 are inequivalent for spin up and spin down states. The inequivalent DOS for spin up and down confirm the magnetic nature of 1T and 1T' phases of CrS_2. More interestingly, the calculated magnetic moment in CrS_2 is affected by the onsite U correction. After adding U correction the magnetic moment per Cr atom for 1T and 1T' phase of CrS_2 change from 0.012 to 0.531μ_B and 0 μ_B to 2.206 μ_B respectively (Table S4).

Table S4. Relative total energy (ΔE) with respect to the most stable configuration calculated with the same functional, magnetic moment per Cr atom

Functional	**Phase**	**ΔE (eV/CrS_2)**	**Mag. mom (μ_B)**
GGA Non-spin polarized	2H	0.0	0
	1T	0.522	0
	1T’	0.370	0
GGA Spin-polarized	2H	0.0	0
	1T	0.524	0.012
	1T’	0.370	0
GGA+(U=2.8)	2H	0.020	0
	1T	0.338	0.531
	1T’	0.0	2.206

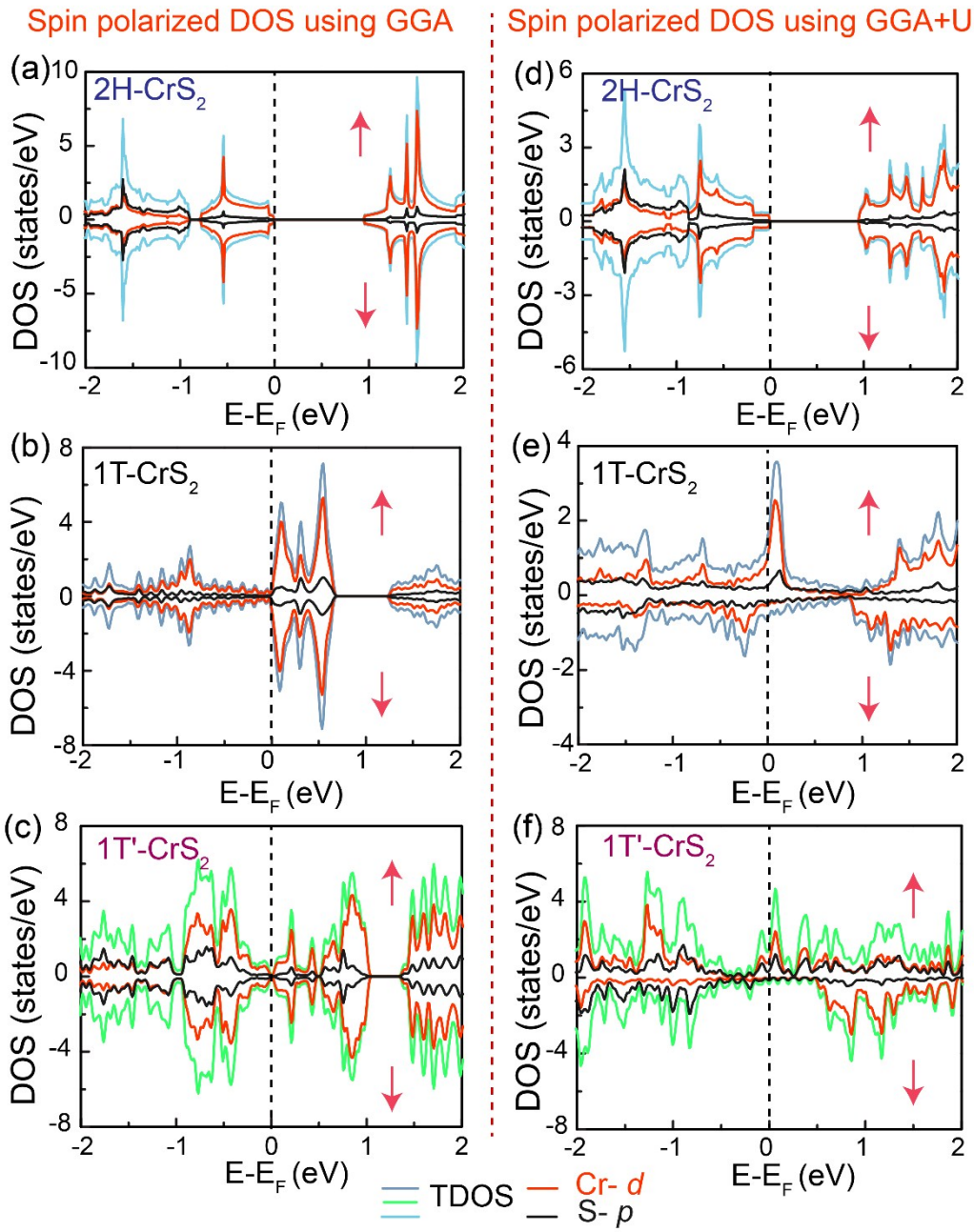

Fig. S17 Spin polarized density of states using GGA functional and GGA+U of (a, d) 2H-CrS_2 (b, e) 1T-CrS2, (c, f) 1T,-CrS_2. Top and bottom arrows denote spin up and spin down channel, respectively.

References:

1. S. Zhou, R. Wang, J. Han, D. Wang, H. Li, L. Gan and T. Zhai, *Adv. Funct. Mater.*, 2019, **29**, 1805880.

2. P. Marcel, D. Mirjana, I.-R. Victor, F. Xavier, C.-G. Andres, P.-T. Amador, M. Narcis, E.-R. Moises, L.-M. Simon, N. Markus, B. Veronica, Y. Anatoliy and P.-R. Alejandro, *2D Mater.*, 2015, **2**, 035006.

3. A. Berkdemir, H. R. Gutiérrez, A. R. Botello-Méndez, N. Perea-López, A. L. Elías, C.-I. Chia, B. Wang, V. H. Crespi, F. López-Urías, J.-C. Charlier, H. Terrones and M. Terrones, *Sci. Rep.*, 2013, **3**, 1755.

4. R. Saito, Y. Tatsumi, S. Huang, X. Ling and M. S. Dresselhaus, *J. Phys.: Condens. Matter*, 2016, **28**, 353002.

5. K. Refson, P. R. Tulip and S. J. Clark, *Phys. Rev. B*, 2006, **73**, 155114.

6. P. Vajeeston, P. Ravindran and H. Fjellvåg, *J. Phys. Chem. A*, 2011, **115**, 10708-10719.

7. Y. Yu, G.-H. Nam, Q. He, X.-J. Wu, K. Zhang, Z. Yang, J. Chen, Q. Ma, M. Zhao, Z. Liu, F.-R. Ran, X. Wang, H. Li, X. Huang, B. Li, Q. Xiong, Q. Zhang, Z. Liu, L. Gu, Y. Du, W. Huang and H. Zhang, *Nat. Chem.*, 2018, **10**, 638-643.

8. *http://www.hqgraphene.com/All-Semiconductors.php*.

9. C. Wang, X. Zhou, Y. Pan, J. Qiao, X. Kong, C.-C. Kaun and W. Ji, *Phys. Rev. B*, 2018, **97**, 245409.

10. H. L. Zhuang, M. D. Johannes, M. N. Blonsky and R. G. Hennig, *Appl. Phys. Lett.*, 2014, **104**, 022116.